

# Elliptic flow of heavy flavors

Santosh K Das\* and Jan-e Alam†

Variable Energy Cyclotron Centre, 1/AF, Bidhan Nagar, Kolkata - 700064

(Dated: July 23, 2018)

The propagation of charm and bottom quarks through an ellipsoidal domain of quark gluon plasma has been studied within the ambit of non-equilibrium statistical mechanics. Energy dissipation of heavy quarks by both radiative and collisional processes are taken in to account. The experimental data on the elliptic flow of the non-photonic electrons resulting from the semi-leptonic decays of hadrons containing heavy flavours has been reproduced with the same formalism that has been used earlier to reproduce the nuclear suppression factors. The elliptic flow of the non-photonic electron from heavy meson decays produced in nuclear collisions at LHC and low energy RHIC run have also been predicted.

PACS numbers: 12.38.Mh, 25.75.-q, 24.85.+p, 25.75.Nq

The nuclear collisions at Relativistic Heavy Ion Collider (RHIC) and the Large Hadron Collider (LHC) energies are aimed at creating a phase where the bulk properties of the matter are governed by (light) quarks and gluons. Such a phase of matter is called Quark Gluon Plasma (QGP). The study of the properties of QGP is a field of high current interest. Experimental results already available from RHIC [1] have been successfully described by the application of relativistic hydrodynamics [2, 3] indicating substantial collective dynamics in the system. In a hydrodynamic model one of the key assumption is that the system achieves thermalization. The elliptic flow parameter  $v_2^{HF}$ , is one such quantity which is sensitive to the early thermalization of the system.

As the relaxation time for heavy quarks are larger than the corresponding quantities for light partons [4] the light quarks and the gluons get thermalized faster than the heavy quarks. Therefore, the propagation of heavy quarks through a QGP (mainly containing light quarks and gluons) may be treated as the interactions between equilibrium and non-equilibrium degrees of freedom and the Fokker-Planck (FP) equation provides an appropriate framework [4–13] for such studies. Since heavy quarks remain out of equilibrium *i.e.* they are not a part of the equilibrated system and their production is restricted to the primordial stages of the collision, they can not decide the bulk properties of the system, rather act as an efficient probe to extract information about the system. Therefore, in the present work we will use the elliptic flow of heavy quarks [14–16] as a probe to extract the properties of QGP.

In our earlier works [17], we have used the FP equation to study the experimental results from STAR and PHENIX collaborations on nuclear sup-

pression factor,  $R_{AA}$  of the non-photonic electrons resulting from the semi-leptonic decays of hadrons containing heavy flavours [18, 19]. In the same approach the  $R_{AA}$ 's have been predicted [20, 21] for LHC and low energy RHIC runs [22, 23]. In the present work we intend to study the elliptic flow measured at RHIC energy with the same formalism and input parameters that reproduce the  $R_{AA}$ . The  $v_2^{HF}$  have also been predicted for low energy RHIC and LHC energy.

The FP equation and the procedure adopted in evaluating the drag and diffusion co-efficients are discussed in detail earlier [17, 20, 21]. Therefore, in the present work we outline the main results and refer to the earlier works for details. The evolution of heavy quarks momentum distribution function, while propagating through the QGP are assumed to be governed by the FP equation which reads,

$$\frac{\partial f}{\partial t} = \frac{\partial}{\partial p_i} \left[ A_i(p) f + \frac{\partial}{\partial p_j} [B_{ij}(p) f] \right] \quad (1)$$

where the kernels  $A_i$  and  $B_{ij}$  are given by

$$\begin{aligned} A_i &= \int d^3 k \omega(p, k) k_i \\ B_{ij} &= \int d^3 k \omega(p, k) k_i k_j. \end{aligned} \quad (2)$$

for  $|\mathbf{p}| \rightarrow \mathbf{0}$ ,  $A_i \rightarrow \gamma p_i$  and  $B_{ij} \rightarrow D \delta_{ij}$  where  $\gamma$  and  $D$  stand for drag and diffusion co-efficients respectively. The temperature and the baryonic chemical potential dependence of the transport coefficients enter through the thermal parton distributions [20] which appear in  $\omega(p, k)$  as

$$\omega(p, k) = g \int \frac{d^3 q}{(2\pi)^3} f'(q) v_{\sigma p, q \rightarrow p-k, q+k} \quad (3)$$

The basic inputs required for solving the FP equation are the dissipation co-efficients and initial momentum distributions of the heavy quarks. The drag

\*santosh@vecc.gov.in

†jane@vecc.gov.in

and diffusion coefficients have been evaluated by taking into account both the collisional and radiative processes [21]. In the radiative process the dead cone [24] and Landau-Pomeranchuk-Migdal (LPM) effects are included, the details have been discussed in Ref. [21]. In evaluating the drag and diffusion co-efficients we have used temperature dependent strong coupling,  $\alpha_s$  from [25]. The Debye mass,  $\sim g(T)T$  is also a temperature dependent quantity which is used as a cut-off to shield the infrared divergences arising due to the exchange of massless gluons.

The production of charm and bottom quarks in hadronic collisions is studied extensively [26]. The initial momentum distribution of heavy quarks in pp collisions have been taken from the NLO MNR code [27]. The results from the code may be tested by measuring the production cross sections of heavy mesons (containing  $c$  and  $b$  quarks) in pp collisions at RHIC and LHC energies.

How can the heavy quarks probe the asymmetry of the thermalized system formed by light quarks and gluons? Consider a thermalized ellipsoidal spatial domain of QGP with major and minor axes of lengths  $l_y$  and  $l_x$  (determined by the collision geometry) respectively. Now let us assume that a heavy quark propagates along the major axis then the number of interactions it encounters or in other words the amount of energy it dissipates or the amount of momentum degradation that takes place is different from when it propagates along the minor axis, because  $l_y \neq l_x$ . Therefore, the momentum distribution of electrons originating from the decays of charmed hadrons ( $D$  mesons) produced from the charm quark fragmentation will be anisotropic, thus reflecting the spatial anisotropy due to non-central collisions in the momentum distributions. The degree of momentum anisotropy will depend on both the spatial anisotropy and more importantly on the coupling strength of the interactions between the heavy quark and the QGP. In an extreme case of zero interaction strength the momentum anisotropy will be zero even if the spatial anisotropy is large. For a quantitative understanding we consider the following. The time evolution of the  $i$ th component of the average momentum for an ellipsoidal geometry can be obtained from the expressions:

$$\langle p_i \rangle \sim \exp\left(-\int^{l_i/v} \gamma(t) dt\right) \quad (4)$$

where  $v$  is the velocity of the heavy quark and  $l_i$  is the length along the  $i$ th direction. The eccentricity of the momentum-space ellipse due to anisotropic momentum distribution resulting from

spatial anisotropy as discussed above is given by:

$$\epsilon_p = \frac{\langle p_x^2 \rangle - \langle p_y^2 \rangle}{\langle p_x^2 \rangle + \langle p_y^2 \rangle} \quad (5)$$

where  $\epsilon_p$  is the eccentricity in the momentum space. The values of  $l_y$  and  $l_x$  are fixed by geometry of the collisions and can be estimated using Glauber model for different centralities. Both  $l_x \neq l_y$  and  $\gamma \neq 0$  (non-zero interaction) are required for non-zero elliptic flow. The second Fourier coefficient of the momentum distributions is called elliptic flow,  $v_2^{HF}$  and we evaluate this quantity in the present work.

The FP equation has been solved for the heavy quarks by using the Greens function technique (see [8] for details). The initial  $p_T$  distribution is taken from NLO MNR formalism [27]. We convolute the solution (at the transition point *i.e.* when the QGP reverts back to hadronic phase) with the Peterson fragmentation function [28] of the heavy quarks to obtain the  $p_T$  distribution of the heavy ( $B$  and  $D$ ) mesons. The momentum distribution,  $dN/dydp_Td\phi$  of the non-photon single electron spectra originating from the decays of heavy flavour mesons -  $e.g.$   $D \rightarrow X e \nu$  at mid-rapidity ( $y = 0$ ) is obtained by following the procedure described in [17, 29, 30]. The coefficient of elliptic flow,  $v_2^{HF}$  then can be obtained as:

$$v_2^{HF}(p_T) = \langle \cos(2\phi) \rangle = \frac{\int d\phi \frac{dN}{dydp_Td\phi}|_{y=0} \cos(2\phi)}{\int d\phi \frac{dN}{dydp_Td\phi}|_{y=0}} \quad (6)$$

The system formed in nuclear collisions at relativistic energies evolves dynamically from the initial to the final state. The time evolution of this systems has been studied by using the (2+1) dimensional hydrodynamical model [31] with boost invariance along the longitudinal direction [32]. It is expected that the central rapidity region of the system formed after nuclear collisions at LHC energy is almost net baryon free. Therefore, the equation governing the conservation of net baryon number need not be considered for RHIC and LHC'.

The total amount of energy dissipated by a heavy quark in the QGP depends on the path length it traverses. Each parton traverse different path length which depends on the geometry of the system and on the point where its is created. The probability that a parton is produced at a point  $(r, \phi')$  in a QGP of ellipsoidal shape depends on the number of binary collisions at that point which can be taken as:

$$P(r, \phi') = \frac{1}{N} \left(1 - \frac{r^2}{R^2} \frac{(1 + \epsilon \cos^2 \phi')}{(1 - \epsilon^2)^2}\right) \Theta(R-r) \quad (7)$$

and

$$\mathcal{N} = \frac{1}{\pi R^2 \left(1 - \frac{1}{2} \frac{1+\epsilon^2/2}{(1-\epsilon^2)^2}\right)} \quad (8)$$

where  $R$  is the nuclear radius and  $\epsilon$  is the eccentricity of the ellipse. Note that for central collisions ( $\epsilon = 0$ ) Eq. 7 reduces to the expression for  $P(r, \phi')$  used in Ref. [9] for spherical geometry. A parton created at  $(r, \phi')$  in the transverse plane propagate a distance  $L = \sqrt{R^2 - r^2 \sin^2 \phi'} - r \cos \phi'$  in the medium. We use the following equation for the geometric average of the integral which appear in the solution of the FP equation involving drag coefficient:

$$\Gamma = \frac{\int r dr d\phi' P(r, \phi') \int^{L/v} d\tau \gamma(\tau)}{\int r dr d\phi' P(r, \phi')} \quad (9)$$

where  $v$  is the velocity of the propagating partons. Similar averaging has been performed for the diffusion co-efficient. For a static system the temperature dependence of the drag and diffusion co-efficients of the heavy quarks enter via the thermal distributions of light quarks and gluons through which it is propagating. However, in the present scenario the variation of temperature with time is governed by the equation of state or the velocity of sound of the thermalized system undergoing hydrodynamic expansion. In such a scenario the quantities like  $\Gamma$  (Eq. 9) and hence  $v_2$  becomes sensitive to velocity of sound ( $c_s$ ) in the medium.

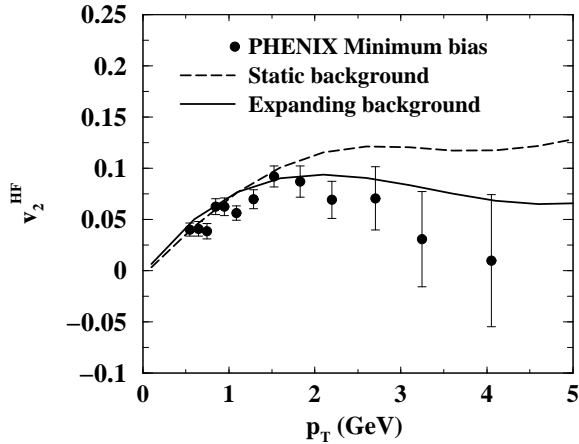


FIG. 1: Variation of  $v_2^{HF}$  with  $p_T$  at the highest RHIC energy. Experimental data is taken from [33].

The  $p_T$  dependence of  $v_2^{HF}$  is sensitive to the nature of the initial distributions of heavy quarks, life time of the system, velocity of sound as well as the drag and diffusion coefficients of heavy quarks.

The experimental data [33] at RHIC energy ( $\sqrt{s_{NN}}=200$  GeV) shows non-zero elliptic flow in-

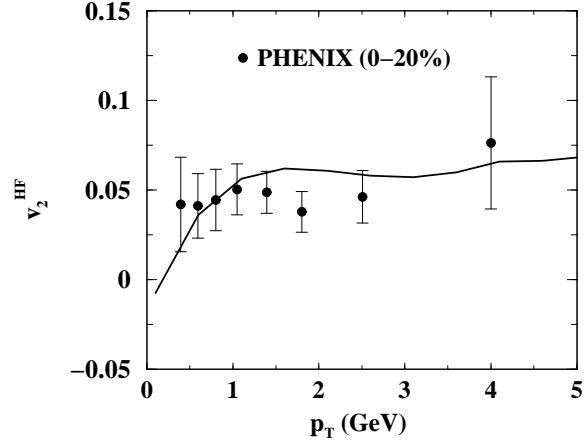


FIG. 2: Same as Fig. 1 for 0-20% centrality. Experimental data contain both the statistical and systematic errors, taken from [37].

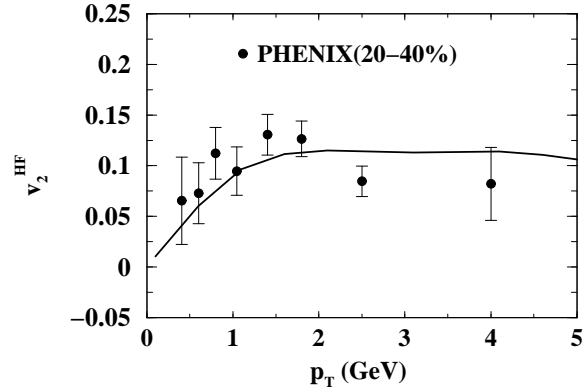


FIG. 3: Same as Fig. 1 for 20-40% centrality. Experimental data contain both the statistical as well as systematic errors, taken from [37].

dicating substantial interactions of the plasma particles with charm and bottom quarks from which electrons are originated through the process:  $c(b)$  (hadronization)  $\rightarrow D(B)$ (decay)  $\rightarrow e+X$ . In Fig. 1 we compare the experimental data obtained by the PHENIX [33] collaborations for Au + Au minimum bias collisions at  $\sqrt{s_{NN}} = 200$  GeV with theoretical results obtain in the present work. We observe that the data can be reproduced by considering both radiative and collisional loss with  $c_s = 1/\sqrt{4}$ . In this case  $v_2^{HF}$  first increases and reaches a maximum of about 8% then saturates for  $p_T > 2$  GeV. From the energy dissipation we have evaluated the shear viscosity ( $\eta$ ) to entropy ( $s$ ) density ratio using the relation [34]:  $\eta/s \sim 1.25T^3/\hat{q}$ , where  $\hat{q} = \langle p_T^2 \rangle / L$  and  $dE/dx \sim \alpha_s \langle p_T^2 \rangle$  [35],  $L$  is the length traversed by the heavy quark and  $p_T$  is its transverse momentum.

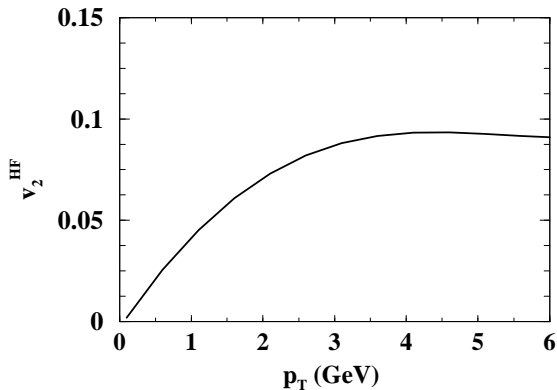


FIG. 4: The variation of  $v_2^{HF}$  with  $p_T$  for LHC initial conditions for 0-10% centrality.

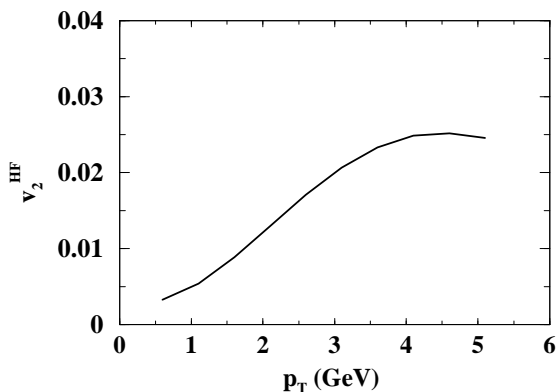


FIG. 5: The variation of  $v_2^{HF}$  with  $p_T$  for low energy RHIC initial conditions for 0-10% centrality.

The average value of  $\eta/s \sim 0.1 - 0.2$ , slightly above the AdS/CFT bound [36]. In Fig. 1 we also display the results obtained when the expansion of the background matter is switched off (dashed line). In this case values of the drag and diffusion co-efficients are evaluated at the initial temperature. The magnitude of  $v_2$  is more when background is static, the reason for this can be understood from the following. The  $v_2$  controls the length of the major axis ( $= 1 + v_2$ ) and minor axis ( $= 1 - v_2$ ) and therefore, it also determine the value of the eccentricity as follows:

$$\epsilon_p = \sqrt{1 - \frac{(1 - v_2)^2}{(1 + v_2)^2}} \quad (10)$$

Eliminating  $\epsilon_p$  from Eqs. 5 and 10 we can write

$$v_2 = \left[ \frac{\sqrt{\langle p_x^2 \rangle} - \sqrt{\langle p_y^2 \rangle}}{\sqrt{\langle p_x^2 \rangle} + \sqrt{\langle p_y^2 \rangle}} \right]^2 \quad (11)$$

Absence of expansion of the background matter is unable to smoothed out the prevailing momentum anisotropy ( $\langle p_x^2 \rangle \neq \langle p_y^2 \rangle$ ) in the system hence a larger value of  $v_2$  is obtained for a static system as indicated by Eq. 11. The difference between the dashed and solid lines in Fig. 1 also indicates the role of the expansion of the background vis-a-vis initial geometric anisotropy. We would like to mention that except the results indicated by dashed line in Fig. 1 all other results are obtained with the background expansion within the ambit of (2+1) dimensional hydrodynamics.

The comparison of results obtained in the present work with the experimental data [37] obtained for two different centralities are depicted in Figs. 2 and 3. The agreement is reasonable both for 0–20% and 20–40% centralities.

The  $v_2^{HF}$  (for 0-10% centrality collision) at LHC energy has been obtained by using the current formalism is displayed in Fig. 4. The variation of  $v_2^{HF}$  with  $p_T$  is similar to that of RHIC.

Now we turn to collisions at low energy,  $\sqrt{s_{NN}} = 39$  GeV. For the initial conditions the  $p_T$  distribution of heavy quarks in  $pp$  collisions is required. At low collision energy rigorous QCD based calculations for heavy flavour production is not available. In the present work this is obtained from pQCD calculation [38, 39] for the processes:  $gg \rightarrow Q\bar{Q}$  and  $q\bar{q} \rightarrow Q\bar{Q}$ . The composition of the matter formed at low energy collisions will be different from that of the matter formed at highest RHIC/LHC energies. The net baryon number will be non-zero for low energy collisions. Therefore, in addition to temperature we need another thermodynamic variable, the baryonic chemical potential,  $\mu_B$  to characterize the matter. As a result in addition to energy momentum conservation equation which is used to study the evolution of baryon free matter we need to solve the baryon number conservation equation also. More details about the initial conditions,  $T$  and  $\mu_B$  dependence of the transport coefficients and the space time evolution have been outlined in [20].

At low  $\sqrt{s_{NN}} (= 39$  GeV) the net baryon density at mid-rapidity is non-zero and its value could be high depending on the value of  $\sqrt{s_{NN}}$ . Therefore, we need to solve the FP equation for both non-zero  $T$  and  $\mu_B$  which enters the equation through the drag and diffusion coefficients. The baryonic chemical potential for  $\sqrt{s_{NN}} = 39$  GeV has been obtained from the parametrization of the experimental data on hadronic ratios as [40] (see also [41]),

$$\mu_B(s_{NN}) = a(1 + \sqrt{s_{NN}}/b)^{-1} \quad (12)$$

where  $a = 0.967 \pm 0.032$  GeV and  $b = 6.138 \pm 0.399$  GeV. The parametrization in Eq. 12 gives the values of  $\mu_B$  at the freeze-out. The corresponding value

at the initial condition is obtained from the baryon number conservation equation.

In Fig. 5,  $v_2^{HF}$  for  $\sqrt{s_{NN}} = 39$  GeV has been displayed. The lack of saturation in the trend of  $v_2^{HF}$  reflect insignificant B-meson contribution as well as the short life time of the plasma.

So far we have discussed the azimuthal asymmetries of the non-photonic electron produced in nuclear collisions due to the propagation of the heavy quark in the partonic medium in the pre-hadronization era. However, the azimuthal asymmetries of the D mesons in the post hadronization era (when both the temperature and density are lower than the partonic phase) should in principle be also taken into account. The suppression of the D mesons in the post hadronization era is found to be negligibly small [20], indicating the fact that the hadronic medium (of pions and nucleons) is unable to drag the D mesons. In the same spirit we have neglected the azimuthal asymmetries due to the hadronic interactions.

In summary, we have evaluated the azimuthal asymmetries ( $v_2^{HF}$ ) using the Fokker-Planck equation with the same set of inputs that reproduces the nuclear suppression,  $R_{AA}$  measured experimentally

at the highest RHIC energy. We found that the  $B$  meson suffer less flow than  $D$  mesons. The B-meson contribution reflects itself by the saturation of  $v_2^{HF}$  in both LHC and RHIC energy and lack of this trend in low energy RHIC run reflect the insignificant contribution of B-meson. The flow pattern at LHC is similar to that of RHIC. Some comments on the  $R_{AA}$  vis-a-vis  $v_2$  flow are in order here. The  $R_{AA}$  contains the ratio of  $p_T$  distribution of electron resulting from Au+Au to p+p collisions, where the numerator contains the interaction of the heavy quarks with the medium (QGP) and such interactions are absence in the denominator. Whereas for  $v_2$  both the numerator and the denominator contain the interactions with the medium, resulting in some sort of cancellation. Therefore, the  $R_{AA}$  will be sensitive to the  $K$  factor but one should not expect the same kind of sensitivity in  $v_2$ .

**Acknowledgment:** This work is supported by DAE-BRNS project Sanction No. 2005/21/5-BRNS/2455. We are grateful to Matteo Cacciari for providing us the heavy quarks transverse momentum distribution for pp collisions. We are also thankful to Victor Roy for useful discussions on (2+1) dimensional hydrodynamics.

- 
- [1] I. Arsene *et al.* (BRAHMS Collaboration), Nucl. Phys. A **757**, 1 (2005); B. B. Back *et al.* (PHOBOS Collaboration), Nucl. Phys. A **757**, 28 (2005); J. Adams *et al.* (STAR Collaboration), Nucl. Phys. A **757**, 102 (2005); K. Adcox *et al.* (PHENIX Collaboration), Nucl. Phys. A **757**, 184,(2005).
- [2] P. Huovinen and P. V. Ruuskanen, Ann. Rev. Nucl. Part. Sci. **56**, 163 (2006).
- [3] D. A. Teaney, arXiv:0905.2433 [nucl-th].
- [4] G. D. Moore and D. Teaney, Phys. Rev. C **71**, 064904 (2005).
- [5] J. Alam, S. Raha and B. Sinha, Phys. Rev. Lett. **73**, 1895 (1994).
- [6] S. Chakraborty and D. Syam, Lett. Nuovo Cim. **41**, 381 (1984).
- [7] B. Svetitsky, Phys. Rev. D **37**, 2484( 1988).
- [8] H. van Hees, R. Rapp, Phys. Rev. C,**71**, 034907 (2005).
- [9] S. Turbide, C. Gale, S. Jeon and G. D. Moore, Phys. Rev. C **72**, 014906 (2005).
- [10] J. Bjoraker and R. Venugopalan, Phys. Rev. C **63**, 024609 (2001).
- [11] P. Roy, J. Alam, S. Sarkar, B. Sinha and S. Raha, Nucl. Phys. A **624**, 687 (1997)
- [12] M G. Mustafa and M. H. Thoma, Acta Phys. Hung. A **22**, 93 (2005).
- [13] P. Roy, A. K. Dutt-Mazumder and J. Alam, Phys. Rev. C **73**, 044911 (2006).
- [14] H. van Hees, V. Greco, R. Rapp, Phys. Rev. C,**73**, 034913 (2006).
- [15] P. B. Gossiaux, and J. Aichelin, Phys. Rev. C,**78**, 014904 (2008)
- [16] Y. Akamatsu, T. Hatsuda and T. Hirani, Phys. Rev. C **79**, 054907 (2009)
- [17] S. K Das, J. Alam and P. Mohanty, Phys. Rev. C **80**, 054916 (2009)
- [18] B. I. Abeleb *et al.* (STAR Collaboration), Phys. Rev. Lett. **98**, 192301 (2007).
- [19] S. S. Adler *et al.* (PHENIX Collaboration), Phys. Rev. Lett. **96**, 032301 (2006).
- [20] S. K Das, J. Alam, P. Mohanty and B. Sinha Phys. Rev. C **81**, 044912 (2010).
- [21] S. K Das, J. Alam and P. Mohanty, Phys. Rev. C **82**, 014908 (2010).
- [22] T. Sakaguchi (PHENIX collaboration), arXiv:0908.3655 [hep-ex].
- [23] B. I. Abelev (Star Collaboration), arXiv:0909.4131 [nucl-ex]
- [24] Y. L. Dokshitzer and D. E. Kharzeev, Phys. Lett. B, **519**, 199 (2001).
- [25] O. Kaczmarek and F. Zantow, Phys. Rev. D, **71**, 114510 (2005).
- [26] M. Cacciari, S. Frixione, M.L. Mangano, P. Nason and G. Ridolfi, J. High Ener. Phys. **0407**, 033 (2004); M. Cacciari and P. Nason, Phys. Rev. Lett. **89**, 122003 (2002); M. Cacciari and P. Nason, J. High Ener. Phys. **0309**, 006 (2003); M. Cacciari, P. Nason and R. Vogt, Phys. Rev. Lett. **95**, 122001 (2005).
- [27] M. L. Mangano, P. Nason and G. Ridolfi, Nucl. Phys. B **538**, 282 (2002).
- [28] C. Peterson *et al.*, Phys. Rev. D **27**, 105 (1983).

- [29] M. Gronau, C. H. Llewellyn Smith, T. F. Walsh, S. Wolfram and T. C. Yang, Nucl. Phys. B **123**, 47 (1977).
- [30] A. Ali, Z. Phys. C **1**, 25 (1979)
- [31] P. F. Kolb, J. Sollfrank and U. Heinz, Phys. Rev. C **62**, 054909 (2000); P. F. Kolb and R. Rapp, Phys. Rev. C **67**, 044903 (2003); P. F. Kolb and U. Heinz, nucl-th/0305084, J. Sollfrank, P. Koch and U. Heinz, Phys. Lett. B **252**, 256 (1990) J. Sollfrank, P. Koch and U. Heinz, Z. Phys. C **52**, 593 (1991).
- [32] J. D. Bjorken, Phys. Rev. D **27**, 140 (1983).
- [33] S. S. Adler *et al.* (PHENIX Collaboration), Phys. Rev. Lett. **98**, 172301 (2007)
- [34] A. Majumder, B. Müller and X. N. Wang, Phys. Rev. Lett. **99**, 192301 (2007).
- [35] R. Baier, arXiv hep-ph/0209038.
- [36] P. Kovtun, D. T. Son and A. O. Starinets, Phys. Rev. Lett. **94**, 111601 (2005).
- [37] A. Adare *et al.* (PHENIX Collaboration), arXiv 1005.1627[nucl-ex].
- [38] R. D. Field, Application of Perturbative QCD, Addison-Wesley Pub. Company, N.Y. 1989.
- [39] B.L. Combridge, Nucl.Phys.B **151**, 429 (1979).
- [40] O. Ristea (for the BRAHMS collaboration) Romanian Reports in Physics, **56**, 659(2004)
- [41] A. Andronic, P. Braun-Munzinger and J. Stachel, Nucl. Phys. A **772**, 167 (2006).